Electronic Supplementary Information

Janus silver/ternary silver halide nanostructures as plasmonic photocatalysts boost the conversion of CO_2 to acetaldehyde

Henglei Jia,*[†,#] Yanrong Dou,[†,#] Yuanyuan Yang,[†] Fan Li,[†] and Chun-yang Zhang*[,†]

[†] College of Chemistry, Chemical Engineering and Materials Science, Collaborative Innovation Center of Functionalized Probes for Chemical Imaging in Universities of Shandong, Key Laboratory of Molecular and Nano Probes, Ministry of Education, Shandong Provincial Key Laboratory of Clean Production of Fine Chemicals, Shandong Normal University, Jinan 250014, China

Supplementary Figures

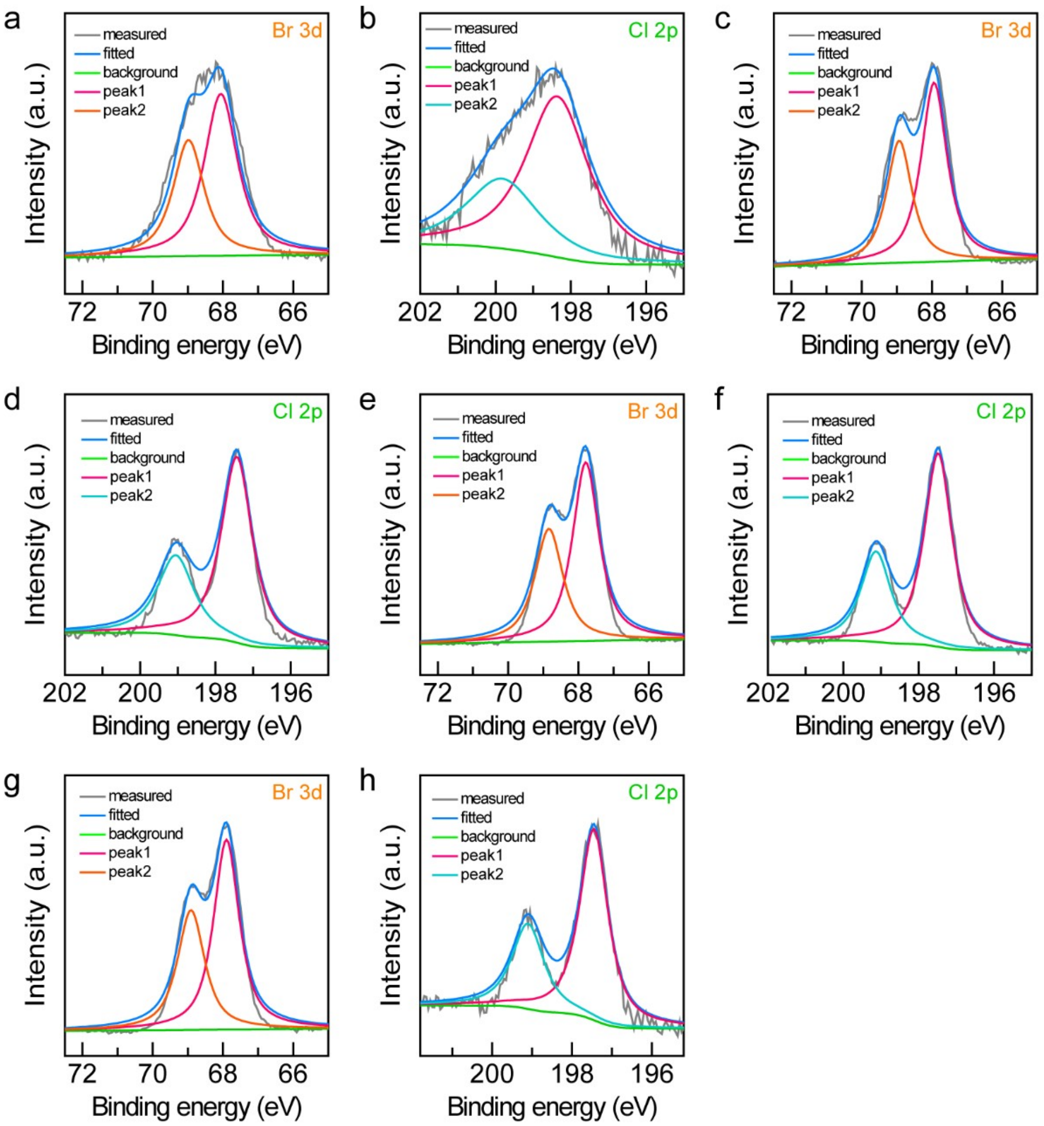

Figure S1. High resolution Br 3d and Cl 2p XPS spectra of the Janus Ag/AgClBr nanostructures when the molar ratios of Br to Cl in the precursors are (a, b) 4:6, (c, d) 5:5, (e, f) 6:4, and (g, h) 8:2, respectively.

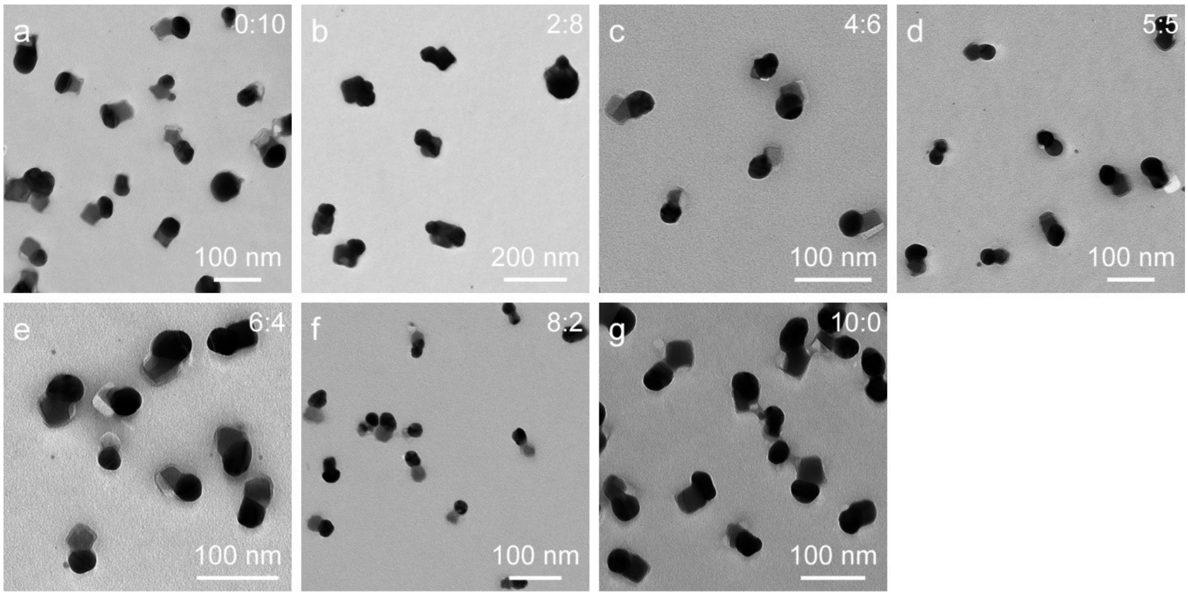

Figure S2. TEM images of the as-obtained Janus Ag/AgX nanostructures with different Cl/Br molar ratios in the precursors: (a) 0:10. (b) 2:8. (c) 4:6. (d) 5:5. (e) 6:4. (f) 8:2. (g) 10:0.

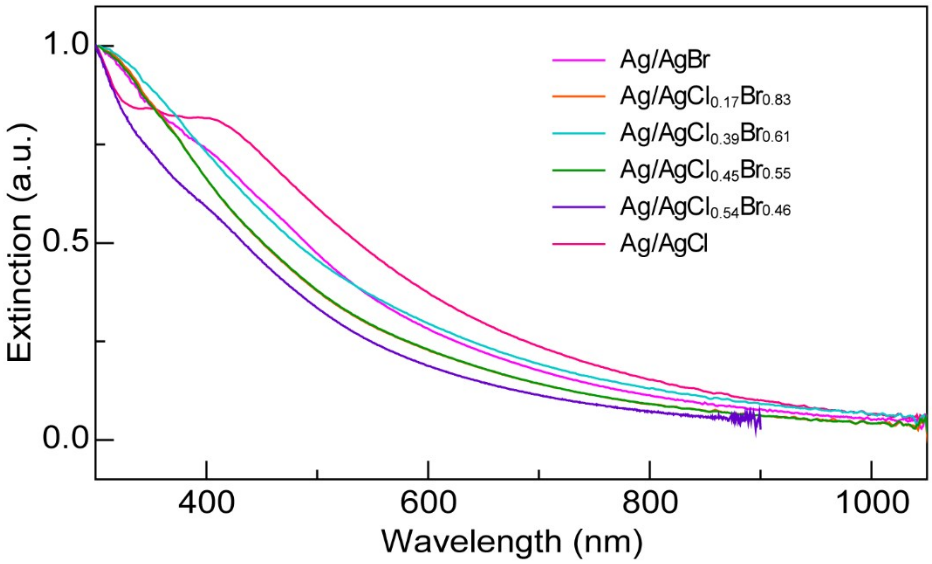

Figure S3. Extinction spectra of the as-obtained Janus Ag/AgX nanostructures with different Cl/Br molar ratios.

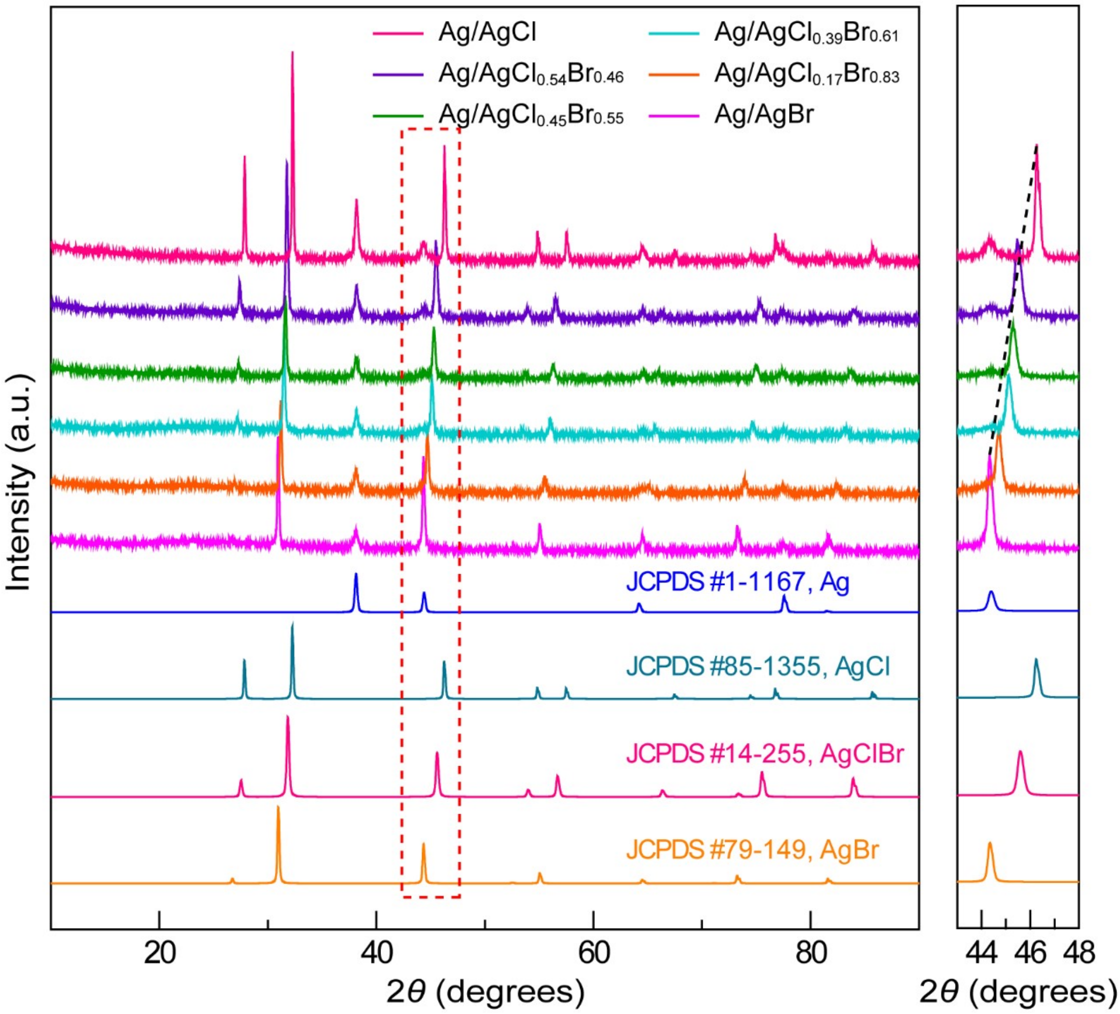

Figure S4. XRD patterns of the as-obtained Janus Ag/AgX nanostructures with different Cl/Br molar ratios. The right figure is the enlarged region marked by dashed red box in the left figure. The four curves (JCPDS #1-1167, Ag; JCPDS #85-1355, AgCl; JCPDS #14-255, AgClBr; JCPDS #79-149, AgBr) are the standard powder diffraction patterns of the face-centered-cubic structure of Ag (space group, F*m*-3*m*; lattice constant, 0.408 nm), the face-centered-cubic structure of AgCl (space group, F*m*-3*m*; lattice constant, 0.5549 nm), the face-centered-cubic structure of AgClBr (space group, F*m*-3*m*; lattice constant, 0.5626 nm), and the face-centered-cubic structure of AgBr (space group, F*m*-3*m*; lattice constant, 0.5775 nm), respectively.

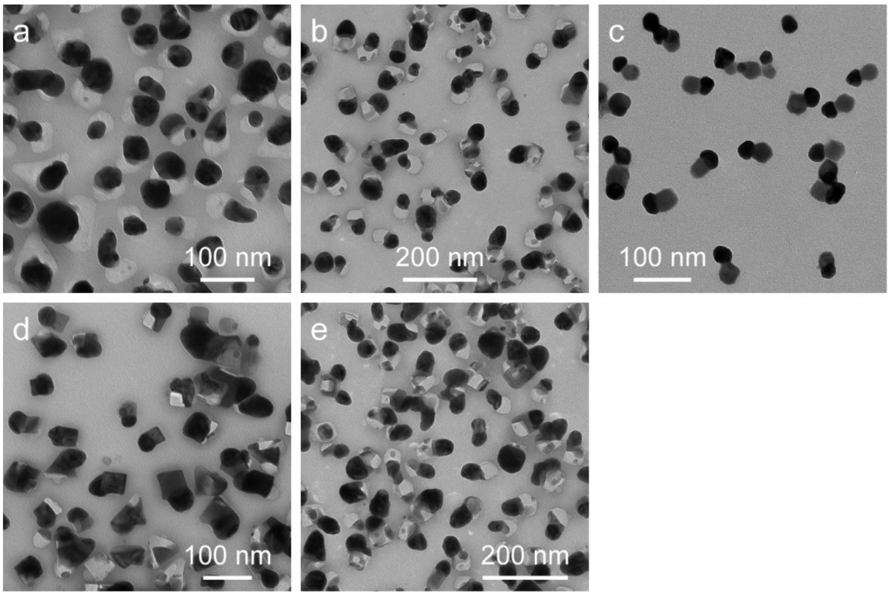

Figure S5. TEM images of the as-obtained Janus Ag/AgX nanostructures with different Ag/X molar ratios in the precursors: (a) 1:4. (b) 1:2. (c) 1:1. (d) 3:2. (e) 2:1.

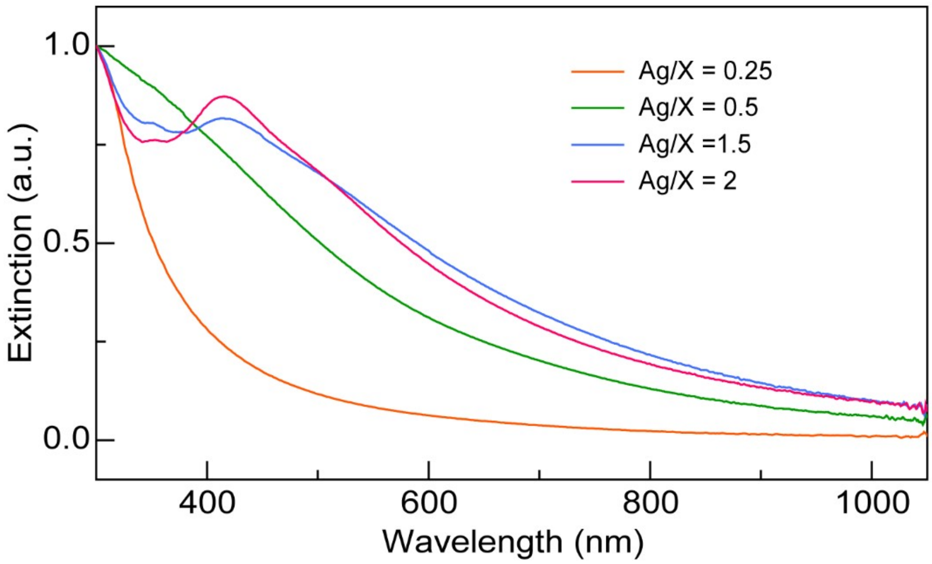

Figure S6. Extinction spectra of the as-obtained Janus Ag/AgX nanostructures with different Ag/X molar ratios in the precursors.

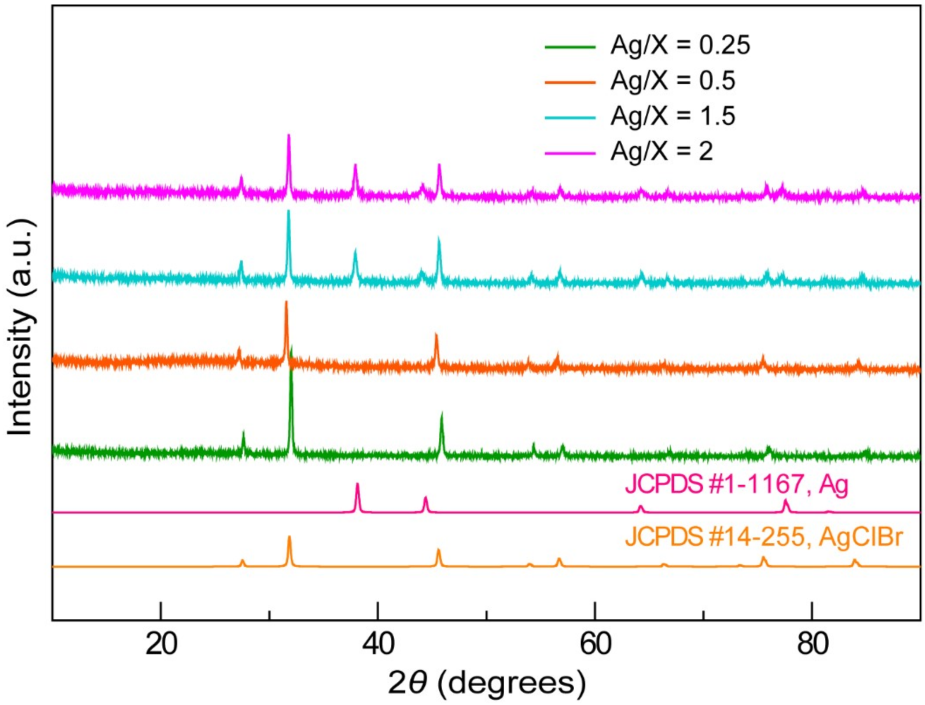

Figure S7. XRD patterns of the as-obtained Janus Ag/AgX nanostructures with different Ag/X molar ratios in the precursors. The red and orange curves (JCPDS #1-1167, Ag; JCPDS #14-255, AgClBr) are the standard powder diffraction patterns of the face-centered-cubic structure of Ag (space group, F*m*-3*m*; lattice constant, 0.408 nm), and the face-centered-cubic structure of AgClBr (space group, F*m*-3*m*; lattice constant, 0.5626 nm).

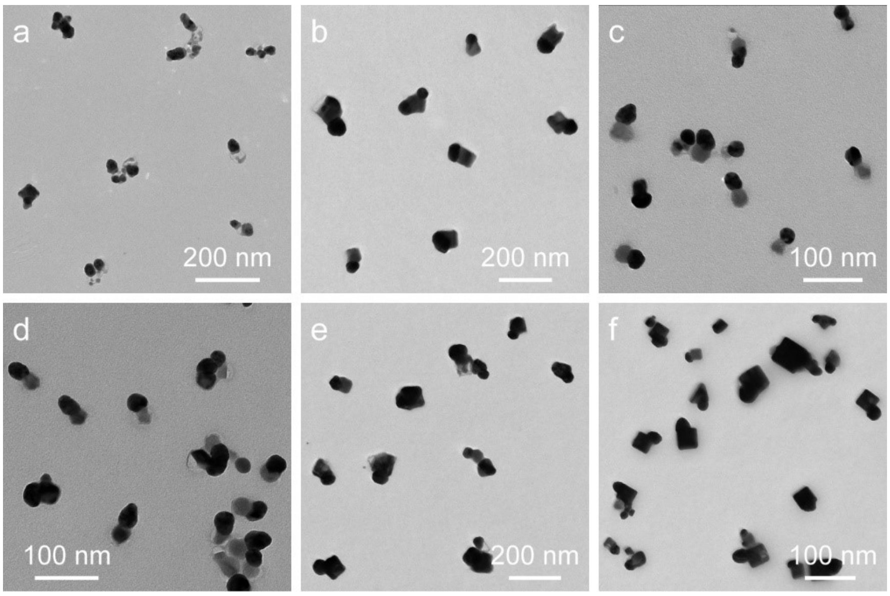

Figure S8. TEM images of the Janus Ag/AgX nanostructures obtained at different injection rates of $AgNO_3$: (a) 0.2 mL·min^{-1}. (b) 0.4 mL·min^{-1}. (c) 0.6 mL·min^{-1}. (d) 0.8 mL·min^{-1}. (e) 1.0 mL·min^{-1}. (f) 1.5 mL·min^{-1}.

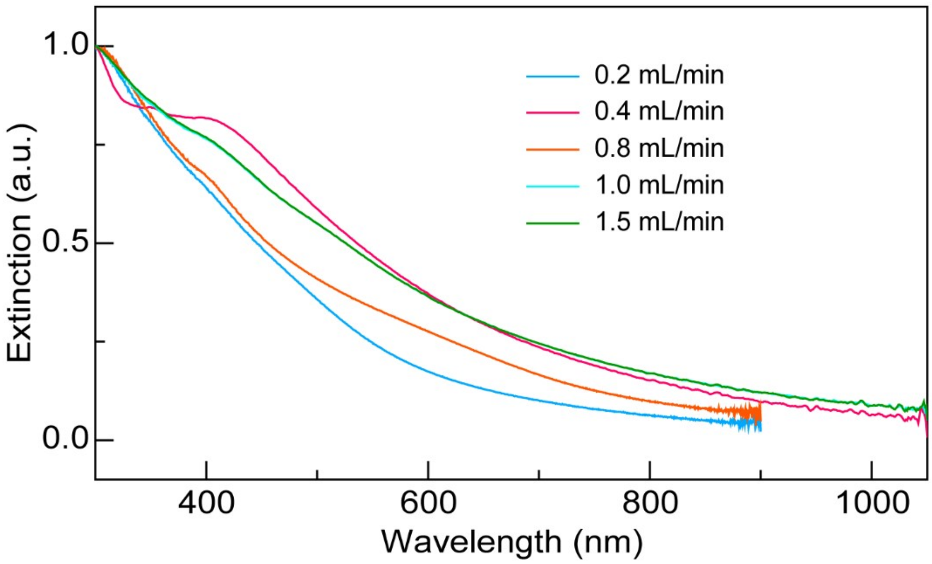

Figure S9. Extinction spectra of the Janus Ag/AgX nanostructures obtained at different injection rates of $AgNO_3$.

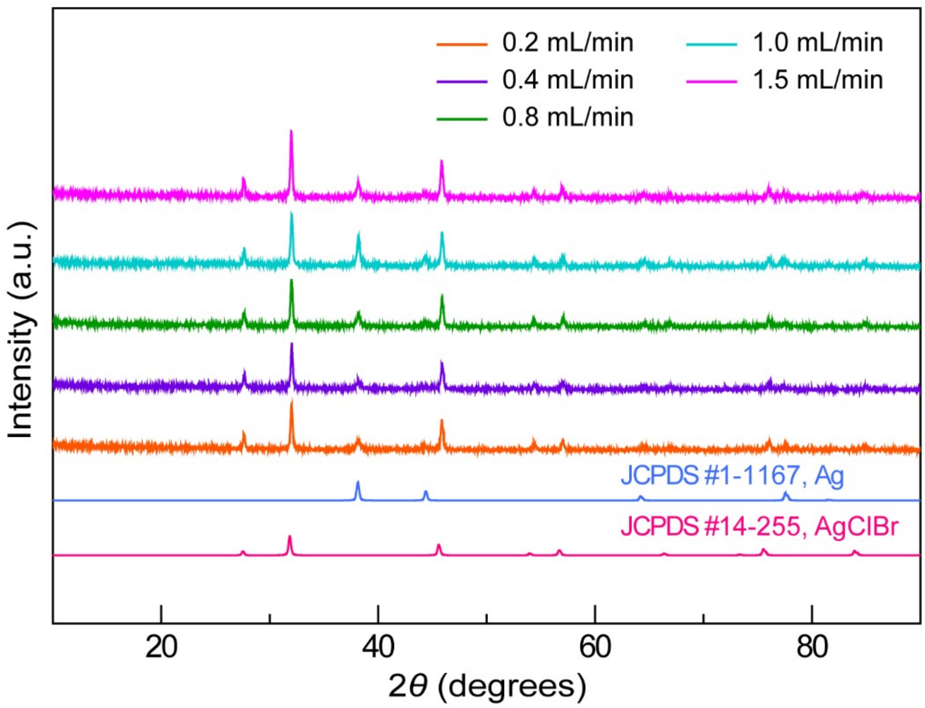

Figure S10. XRD patterns of the Janus Ag/AgX nanostructures obtained at different injection rates of $AgNO_3$. The blue and red curves (JCPDS #1-1167, Ag; JCPDS #14-255, AgClBr) are the standard powder diffraction patterns of the face-centered-cubic structure of Ag (space group, F*m*-3*m*; lattice constant, 0.408 nm), and the face-centered-cubic structure of AgClBr (space group, F*m*-3*m*; lattice constant, 0.5626 nm).

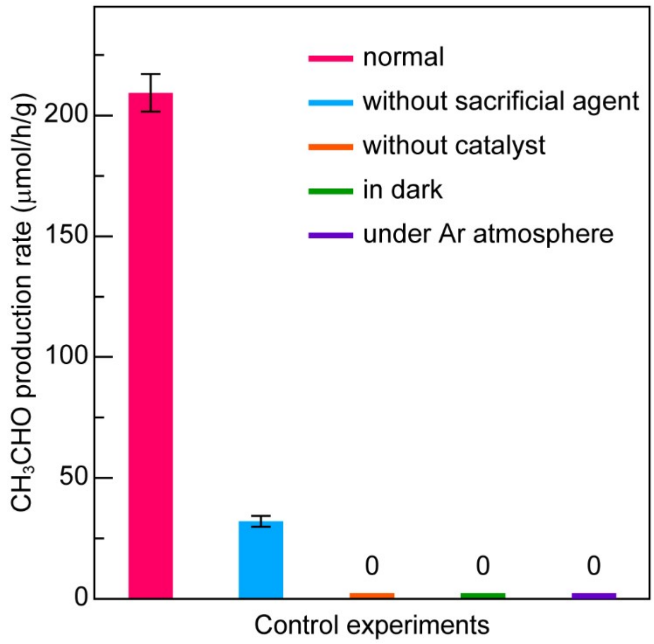

Figure S11. Control experiments of the photocatalytic CO_2 reduction under different conditions.

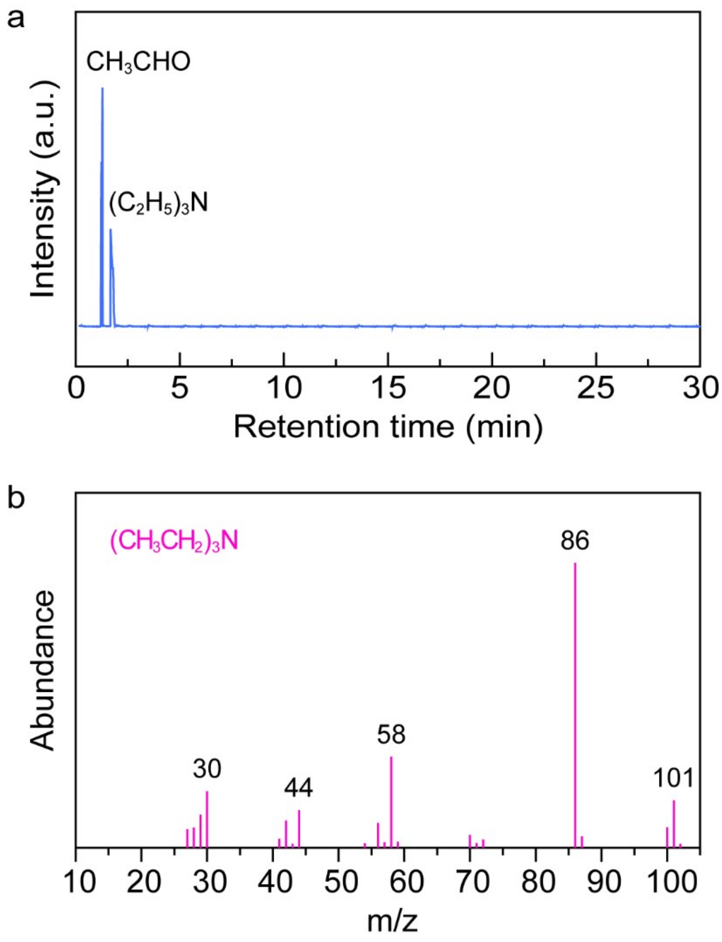

Figure S12. (a) Gas chromatography spectra of the reaction solution after 2-h photocatalytic experiment using the Janus Ag/$AgCl_{0.79}Br_{0.21}$ nanostructures as the catalyst. (b) Mass spectra extracted from the GC–MS analysis of $(CH_3CH_2)_3N$.

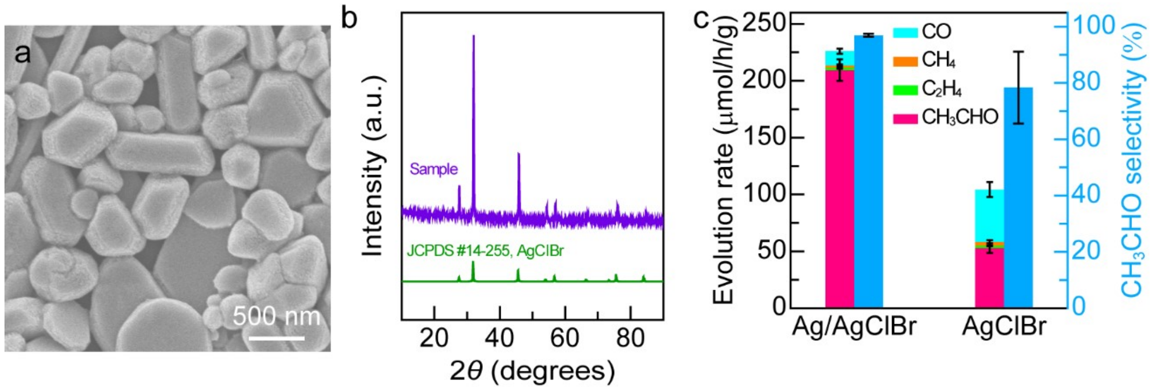

Figure S13. (a) SEM image and (b) XRD patterns of AgClBr nanoparticles. (c) Comparison of photocatalytic performance toward the reduction of CO_2 using the Ag/AgClBr and AgClBr samples as the catalysts.

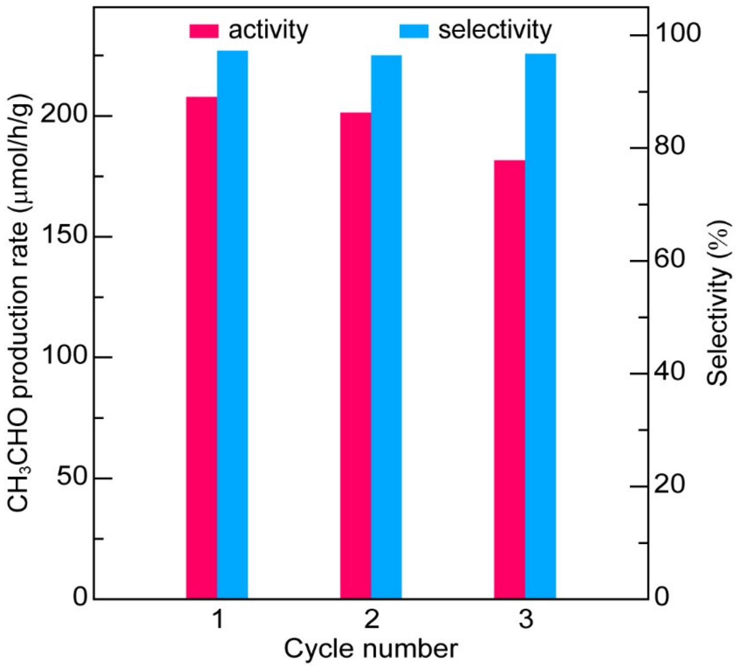

Figure S14. Photocatalytic activity and selectivity toward acetaldehyde generation through the CO_2 reduction during three successive cycles with the Janus Ag/$AgCl_{0.79}Br_{0.21}$ nanostructures as the catalysts.

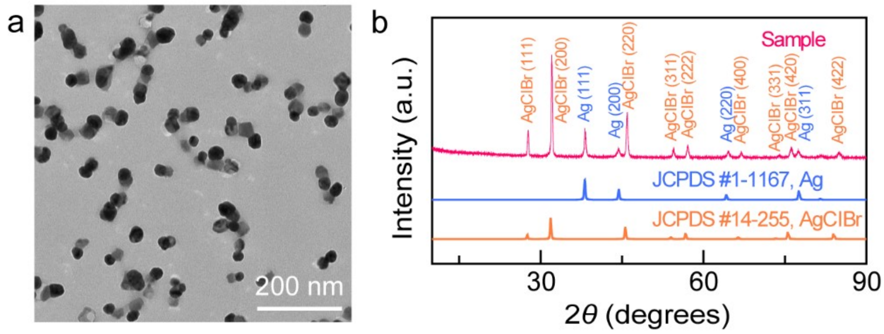

Figure S15. TEM image (a) and XRD patterns (b) of the Janus Ag/$AgCl_{0.79}Br_{0.21}$ nanostructures after the photocatalytic CO_2 reduction reaction.

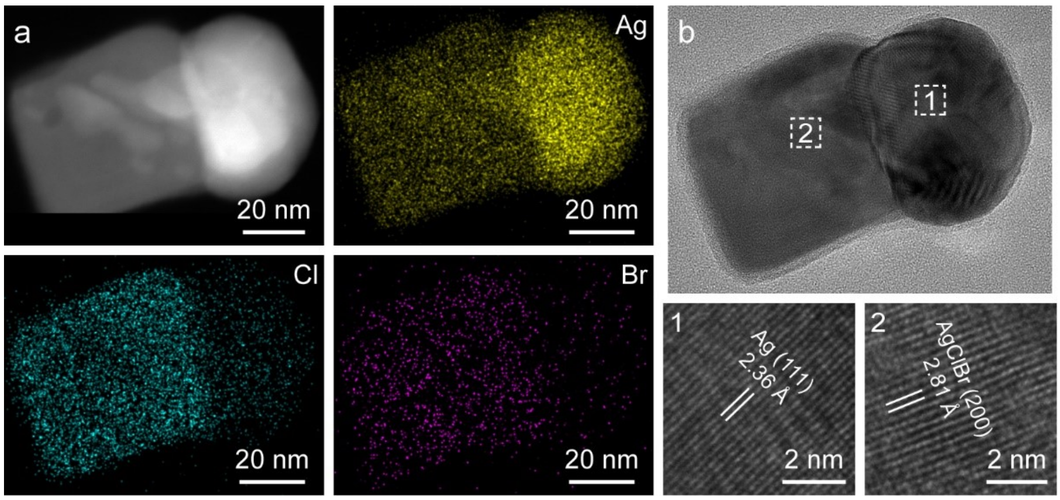

Figure S16. HAADF-STEM image (top-left) and the corresponding EDX maps (a) and HRTEM image (b) of the Janus Ag/$AgCl_{0.79}Br_{0.21}$ nanostructures after the photocatalytic CO_2 reduction reaction.

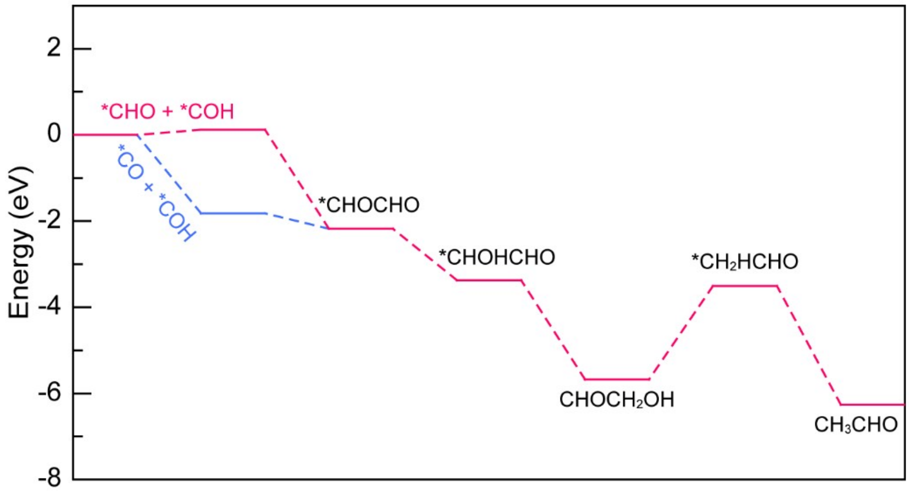

Figure S17. Gibbs free energy diagrams for C–C coupling to CH_3CHO on the Janus Ag/$AgCl_{0.79}Br_{0.21}$ nanostructures.

Table S1. Molar ratios of Cl to Br in different Janus Ag/AgClBr nanostructures.

Sample	$Ag/AgCl_{0.79}Br_{0.21}$	$Ag/AgCl_{0.54}Br_{0.46}$	$Ag/AgCl_{0.45}Br_{0.55}$	$Ag/AgCl_{0.39}Br_{0.61}$	$Ag/AgCl_{0.17}Br_{0.83}$
Cl/Br molar ratios in the precursors	8:2	6:4	5:5	4:6	2:8
Cl/Br molar ratios determined by XPS	0.79/0.21	0.54/0.46	0.45/0.55	0.39/0.61	0.17/0.83

Table S2. Comparison of the photocatalytic CO_2 reduction performance toward the CH_3CHO production among representative works.

catalyst	light source	catalyst amount (mg)	CH_3CHO production rate ($\mu mol \cdot h^{-1} \cdot g^{-1}$)	reference
Cu/graphene oxide	visible light, 100 $mW \cdot cm^{-2}$	100	3.88	*Nano Lett.*, 2014, **14**, 6097.
SnS–SnS_2 nanosheets	AM 1.5G, 100 $mW \cdot cm^{-2}$	–	11.5	*ACS Appl. Mater. Interfaces*, 2021, ***13***, 4984.
NiO/$InTaO_4$ layer	AM 1.5G, 100 $mW \cdot cm^{-2}$	–	0.3	*Energy Environ. Sci.*, 2011, **4**, 1487.
ultrafine $ZnFe_2O_4$ nanoparticles	visible light	20	57.8	*J. Mater. Sci. Technol.*, 2018, **34**, 2331.
Nb-doped TiO_2 nanotube array	simulated solar illumination, 200 $mW \cdot cm^{-2}$	50	572	*ACS Appl. Mater. Interfaces*, 2020, **12**, 55982.
g-C_3N_4/CuO@MIL-125(Ti)	simulated sunlight, 32.61 $mW \cdot cm^{-2}$	100	177.2	*Chem. Eng. J.*, 2020, **399**, 125782.
foam-like Cu_2O	UV-vis light	–	8.2	*Sol. Energy*, 2016, **139**, 452.
Pd/Rh/TiO_2 nanoparticles	320–500 nm, 41.62 $mW \cdot cm^{-2}$	109.9	0.21	*Appl. Catal., B*, 2012, **126**, 172.
carbon-doped SnS_2 nanostructures	visible light, (300 W halogen lamp)	100	96.7	*Nat. Commun.*, 2018, **9**, 169.
Janus Ag/AgClBr nanostructures	AM 1.5G, 100 $mW \cdot cm^{-2}$	40	209.3	*this work*